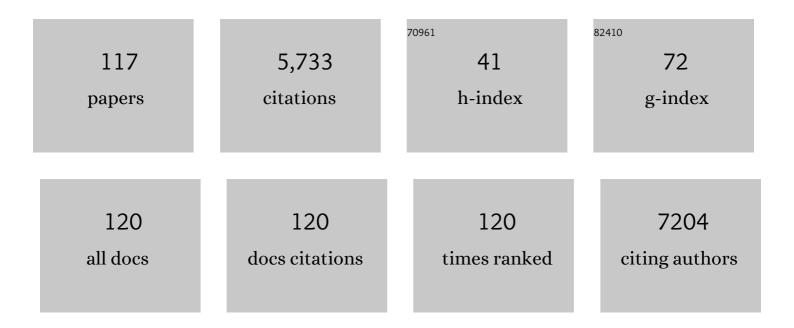
Guowen Meng

List of Publications by Year in descending order

Source: https://exaly.com/author-pdf/5355166/publications.pdf Version: 2024-02-01



#	Article	IF	CITATIONS
1	A Hierarchically Ordered Array of Silverâ€Nanorod Bundles for Surfaceâ€Enhanced Raman Scattering Detection of Phenolic Pollutants. Advanced Materials, 2016, 28, 4871-4876.	11.1	333
2	Arrays of Cone‧haped ZnO Nanorods Decorated with Ag Nanoparticles as 3D Surfaceâ€Enhanced Raman Scattering Substrates for Rapid Detection of Trace Polychlorinated Biphenyls. Advanced Functional Materials, 2012, 22, 218-224.	7.8	312
3	From The Cover: Controlled fabrication of hierarchically branched nanopores, nanotubes, and nanowires. Proceedings of the National Academy of Sciences of the United States of America, 2005, 102, 7074-7078.	3.3	286
4	Catalytic Growth of Large-Scale Single-Crystal CdS Nanowires by Physical Evaporation and Their Photoluminescence. Chemistry of Materials, 2002, 14, 1773-1777.	3.2	221
5	Improved SERS Performance from Au Nanopillar Arrays by Abridging the Pillar Tip Spacing by Ag Sputtering. Advanced Materials, 2010, 22, 4136-4139.	11.1	217
6	Periodically Twinned Nanowires and Polytypic Nanobelts of ZnS:  The Role of Mass Diffusion in Vaporâ^'Liquidâ^'Solid Growth. Nano Letters, 2006, 6, 1650-1655.	4.5	215
7	Controlled Synthesis of In2O3 Octahedrons and Nanowires. Crystal Growth and Design, 2005, 5, 1617-1621.	1.4	170
8	Review—Surface-Enhanced Raman Scattering Sensors for Food Safety and Environmental Monitoring. Journal of the Electrochemical Society, 2018, 165, B3098-B3118.	1.3	147
9	Plasmonic hot electrons for sensing, photodetection, and solar energy applications: A perspective. Journal of Chemical Physics, 2020, 152, 220901.	1.2	141
10	Green Synthesis of Large-Scale Highly Ordered Core@Shell Nanoporous Au@Ag Nanorod Arrays as Sensitive and Reproducible 3D SERS Substrates. ACS Applied Materials & Interfaces, 2014, 6, 15667-15675.	4.0	120
11	Largeâ€area Ag nanorod array substrates for SERS: AAO templateâ€assisted fabrication, functionalization, and application in detection PCBs. Journal of Raman Spectroscopy, 2013, 44, 240-246.	1.2	119
12	Kinetics-Driven Growth of Orthogonally Branched Single-Crystalline Magnesium Oxide Nanostructures. Journal of Physical Chemistry B, 2005, 109, 11204-11208.	1.2	116
13	Ag Nanoparticleâ€Grafted PANâ€Nanohump Array Films with 3D Highâ€Density Hot Spots as Flexible and Reliable SERS Substrates. Small, 2015, 11, 5452-5459.	5.2	112
14	Enhancing potassium-ion battery performance by defect and interlayer engineering. Nanoscale Horizons, 2019, 4, 202-207.	4.1	105
15	Ag nanosheet-assembled micro-hemispheres as effective SERS substrates. Chemical Communications, 2011, 47, 2709-2711.	2.2	101
16	Flexible membranes of Ag-nanosheet-grafted polyamide-nanofibers as effective 3D SERS substrates. Nanoscale, 2014, 6, 4781.	2.8	92
17	Electrospun 1,4-DHAQ-Doped Cellulose Nanofiber Films for Reusable Fluorescence Detection of Trace Cu ²⁺ and Further for Cr ³⁺ . Environmental Science & Technology, 2012, 46, 367-373.	4.6	87
18	Detection of Dithiocarbamate Pesticides with a Spongelike Surface-Enhanced Raman Scattering Substrate Made of Reduced Graphene Oxide-Wrapped Silver Nanocubes. ACS Applied Materials & Interfaces, 2017, 9, 39618-39625.	4.0	80

#	Article	IF	CITATIONS
19	Aligned SiC Porous Nanowire Arrays with Excellent Field Emission Properties Converted from Si Nanowires on Silicon Wafer. Journal of Physical Chemistry C, 2008, 112, 20126-20130.	1.5	77
20	A flexible transparent Ag-NC@PE film as a cut-and-paste SERS substrate for rapid in situ detection of organic pollutants. Analyst, The, 2016, 141, 5864-5869.	1.7	76
21	Highly Sensitive and Selective Surface-Enhanced Raman Spectroscopy Label-free Detection of 3,3′,4,4′-Tetrachlorobiphenyl Using DNA Aptamer-Modified Ag-Nanorod Arrays. ACS Applied Materials & Interfaces, 2016, 8, 5723-5728.	4.0	74
22	Vertically aligned Ag nanoplate-assembled film as a sensitive and reproducible SERS substrate for the detection of PCB-77. Journal of Hazardous Materials, 2012, 211-212, 389-395.	6.5	73
23	Plasmon-tunable Au@Ag core-shell spiky nanoparticles for surface-enhanced Raman scattering. Nano Research, 2019, 12, 449-455.	5.8	72
24	Zn nanobelts: a new quasi one-dimensional metal nanostructure. Chemical Communications, 2001, , 2632-2633.	2.2	71
25	Rational design of novel nanostructured arrays based on porous AAO templates for electrochemical energy storage and conversion. Nano Energy, 2019, 55, 234-259.	8.2	71
26	Tapered Optical Fiber Probe Assembled with Plasmonic Nanostructures for Surface-Enhanced Raman Scattering Application. ACS Applied Materials & Interfaces, 2015, 7, 17247-17254.	4.0	67
27	A General Synthetic Approach to Interconnected Nanowire/Nanotube and Nanotube/Nanowire/Nanotube Heterojunctions with Branched Topology. Angewandte Chemie - International Edition, 2009, 48, 7166-7170.	7.2	66
28	Ag-Nanoparticles@Bacterial Nanocellulose as a 3D Flexible and Robust Surface-Enhanced Raman Scattering Substrate. ACS Applied Materials & Interfaces, 2020, 12, 50713-50720.	4.0	64
29	ZnO-nanotaper array sacrificial templated synthesis of noble-metal building-block assembled nanotube arrays as 3D SERS-substrates. Nano Research, 2015, 8, 957-966.	5.8	62
30	Large-scale well-separated Ag nanosheet-assembled micro-hemispheres modified with HS-Î2-CD as effective SERS substrates for trace detection of PCBs. Journal of Materials Chemistry, 2012, 22, 2271-2278.	6.7	59
31	Gap-tunable Ag-nanorod arrays on alumina nanotip arrays as effective SERS substrates. Journal of Materials Chemistry C, 2013, 1, 5015.	2.7	53
32	Ag-nanoparticle-decorated porous ZnO-nanosheets grafted on a carbon fiber cloth as effective SERS substrates. Nanoscale, 2014, 6, 15280-15285.	2.8	53
33	Color Fineâ€Tuning of CNTs@AAO Composite Thin Films via Isotropically Etching Porous AAO Before CNT Growth and Color Modification by Water Infusion. Advanced Materials, 2010, 22, 2637-2641.	11.1	51
34	Branched Silicon Nanotubes and Metal Nanowires via AAOâ€⊺emplateâ€Assistant Approach. Advanced Functional Materials, 2010, 20, 3791-3796.	7.8	50
35	Aligned ZnO Nanorods with Tunable Size and Field Emission on Native Si Substrate Achieved via Simple Electrodeposition. Journal of Physical Chemistry C, 2010, 114, 189-193.	1.5	50
36	Label-free selective SERS detection of PCB-77 based on DNA aptamer modified SiO2@Au core/shell nanoparticles. Analyst, The, 2014, 139, 3083.	1.7	50

#	Article	IF	CITATIONS
37	Dielectric capacitors with three-dimensional nanoscale interdigital electrodes for energy storage. Science Advances, 2015, 1, e1500605.	4.7	49
38	Controlled Synthesis of Germanium Nanowires and Nanotubes with Variable Morphologies and Sizes. Nano Letters, 2011, 11, 1704-1709.	4.5	48
39	Scalable and controllable fabrication of CNTs improved yolk-shelled Si anodes with advanced in operando mechanical quantification. Energy and Environmental Science, 2021, 14, 3502-3509.	15.6	45
40	Electrochemical synthesis of metal and semimetal nanotube–nanowire heterojunctions and their electronic transport properties. Chemical Communications, 2007, , 1733-1735.	2.2	43
41	Porous AAO template-assisted rational synthesis of large-scale 1D hybrid and hierarchically branched nanoarchitectures. Progress in Materials Science, 2018, 95, 243-285.	16.0	43
42	Y-branched Bi nanowires with metal–semiconductor junction behavior. Applied Physics Letters, 2004, 85, 967-969.	1.5	42
43	A Generic Synthetic Approach to Largeâ€Scale Pristineâ€Graphene/Metalâ€Nanoparticles Hybrids. Advanced Functional Materials, 2013, 23, 5771-5777.	7.8	42
44	Ag-nanoparticles-decorated NiO-nanoflakes grafted Ni-nanorod arrays stuck out of porous AAO as effective SERS substrates. Physical Chemistry Chemical Physics, 2014, 16, 3686.	1.3	39
45	Visible-Light Localized Surface Plasmon Resonance of WO _{3–<i>x</i>} Nanosheets and Its Photocatalysis Driven by Plasmonic Hot Carriers. ACS Sustainable Chemistry and Engineering, 2021, 9, 1500-1506.	3.2	39
46	Enhanced Cold Field Emission of Large-area Arrays of Vertically Aligned ZnO-nanotapers via Sharpening: Experiment and Theory. Scientific Reports, 2014, 4, 4676.	1.6	38
47	Highly sensitive fibre surface-enhanced Raman scattering probes fabricated using laser-induced self-assembly in a meniscus. Nanoscale, 2016, 8, 10607-10614.	2.8	37
48	Reversible blue light emission from self-assembled silica nanocords. Applied Physics Letters, 2005, 87, 033106.	1.5	36
49	Ordered arrays of Au-nanobowls loaded with Ag-nanoparticles as effective SERS substrates for rapid detection of PCBs. Nanotechnology, 2014, 25, 145605.	1.3	36
50	A silver-grafted sponge as an effective surface-enhanced Raman scattering substrate. Sensors and Actuators B: Chemical, 2018, 258, 56-63.	4.0	34
51	Large-scale homogeneously distributed Ag-NPs with sub-10 nm gaps assembled on a two-layered honeycomb-like TiO2film as sensitive and reproducible SERS substrates. Nanotechnology, 2012, 23, 385705.	1.3	33
52	Galvanicâ€Cellâ€Induced Growth of Ag Nanosheetâ€Assembled Structures as Sensitive and Reproducible SERS Substrates. Chemistry - A European Journal, 2012, 18, 14948-14953.	1.7	33
53	Hexagonally arranged arrays of urchin-like Ag hemispheres decorated with Ag nanoparticles for surface-enhanced Raman scattering substrates. Nano Research, 2015, 8, 2261-2270.	5.8	33
54	Au Hierarchical Micro/Nanotower Arrays and Their Improved SERS Effect by Ag Nanoparticle Decoration. Crystal Growth and Design, 2011, 11, 748-752.	1.4	32

#	Article	IF	CITATIONS
55	High-Density, Aligned SiO2Nanowire Arrays:Â Microscopic Imaging of the Unique Growth Style and Their Ultraviolet Light Emission Properties. Journal of Physical Chemistry B, 2006, 110, 15724-15728.	1.2	30
56	Fluorescence detection of trace PCB101 based on PITC immobilized on porous AAO membrane. Analyst, The, 2011, 136, 278-281.	1.7	30
57	Ag-nanoparticle-decorated Au-fractal patterns on bowl-like-dimple arrays on Al foil as an effective SERS substrate for the rapid detection of PCBs. Chemical Communications, 2014, 50, 569-571.	2.2	30
58	Tuning the architecture of MgO nanostructures by chemical vapour transport and condensation. Nanotechnology, 2006, 17, 5006-5012.	1.3	29
59	A Generic Approach to Desired Metallic Nanowires Inside Native Porous Alumina Template via Redox Reaction. Chemistry of Materials, 2009, 21, 2397-2402.	3.2	29
60	Polyacrylic acid sodium salt film entrapped Ag-nanocubes as molecule traps for SERS detection. Nano Research, 2014, 7, 1177-1187.	5.8	29
61	Incorporation of a Basil-Seed-Based Surface Enhanced Raman Scattering Sensor with a Pipet for Detection of Melamine. ACS Sensors, 2016, 1, 1193-1197.	4.0	29
62	Microscopy Study of the Growth Process and Structural Features of Closely Packed Silica Nanowires. Journal of Physical Chemistry B, 2003, 107, 13029-13032.	1.2	28
63	Controlled fabrication of gold and polypyrrole nanowires with straight and branched morphologies via porous alumina template-assisted approach. Materials Letters, 2009, 63, 1431-1434.	1.3	28
64	Prototype of a Porous ZnO SPV-Based Sensor for PCB Detection at Room Temperature under Visible Light Illumination. Langmuir, 2010, 26, 13703-13706.	1.6	24
65	Nanocontainers made of Various Materials with Tunable Shape and Size. Scientific Reports, 2013, 3, 2238.	1.6	23
66	Electrosprayed large-area membranes of Ag-nanocubes embedded in cellulose acetate microspheres as homogeneous SERS substrates. Journal of Materials Chemistry C, 2017, 5, 1402-1408.	2.7	23
67	Silver nanoparticle-assembled micro-bowl arrays for sensitive SERS detection of pesticide residue. Nanotechnology, 2020, 31, 205303.	1.3	23
68	Ag-NP@Ge-nanotaper/Si-micropillar ordered arrays as ultrasensitive and uniform surface enhanced Raman scattering substrates. Nanoscale, 2015, 7, 18218-18224.	2.8	22
69	Nanochannel-Directed Growth of Multi-Segment Nanowire Heterojunctions of Metallic Au _{1–<i>x</i>} Ge _{<i>x</i>} and Semiconducting Ge. ACS Nano, 2012, 6, 831-836.	7.3	21
70	A Hierarchical Nanostructureâ€Based Surfaceâ€Enhanced Raman Scattering Sensor for Preconcentration and Detection of Antibiotic Pollutants. Advanced Materials Technologies, 2017, 2, 1700028.	3.0	20
71	Improved sensitivity of polychlorinated-biphenyl-orientated porous-ZnO surface photovoltage sensors from chemisorption-formed ZnO-CuPc composites. Scientific Reports, 2014, 4, 4284.	1.6	19
72	A Surface-Enhanced Raman Scattering Sensor Integrated with Battery-Controlled Fluidic Device for Capture and Detection of Trace Small Molecules. Scientific Reports, 2015, 5, 12865.	1.6	19

#	Article	IF	CITATIONS
73	Template-assisted fabrication of Ag-nanoparticles@ZnO-nanorods array as recyclable 3D surface enhanced Raman scattering substrate for rapid detection of trace pesticides. Nanotechnology, 2021, 32, 145302.	1.3	19
74	Ag-Nanoparticle-Decorated Ge Nanocap Arrays Protruding from Porous Anodic Aluminum Oxide as Sensitive and Reproducible Surface-Enhanced Raman Scattering Substrates. Langmuir, 2014, 30, 13964-13969.	1.6	18
75	Spinach-extracted chlorophyll-a modified peanut shell as fluorescence sensors for selective detection of Hg2+ in water. Sensors and Actuators B: Chemical, 2015, 209, 237-241.	4.0	18
76	Mesh-Like Hemispherical Shells Formed by Self-Assembly of Zn2SiO4Textured Nanowires. Crystal Growth and Design, 2006, 6, 1967-1971.	1.4	17
77	Synthesis of vertically oriented GaN nanowires on a LiAlO2 substrate via chemical vapor deposition. Nano Research, 2009, 2, 321-326.	5.8	17
78	lodeosin-based fluorescent and colorimetric sensing for Ag ⁺ , Hg ²⁺ , Fe ³⁺ , and further for halide ions in aqueous solution. RSC Advances, 2014, 4, 8055-8058.	1.7	17
79	Fluorophores-modified nanomaterials for trace detection of polychlorobiphenyls and heavy metal ions. Sensors and Actuators B: Chemical, 2017, 243, 1137-1147.	4.0	17
80	Long-range surface plasmon resonance and surface-enhanced Raman scattering on X-shaped gold plasmonic nanohole arrays. Physical Chemistry Chemical Physics, 2017, 19, 24126-24134.	1.3	17
81	CNTs-anchored egg shell membrane decorated with Ag-NPs as cheap but effective SERS substrates. Science China Materials, 2015, 58, 198-203.	3.5	16
82	Crystalline Silicon Nanotubes and Their Connections with Gold Nanowires in Both Linear and Branched Topologies. ACS Nano, 2010, 4, 7105-7112.	7.3	15
83	Fluorophore-modified Fe3O4-magnetic-nanoparticles for determination of heavy metal ions in water. Sensors and Actuators B: Chemical, 2013, 185, 47-52.	4.0	15
84	Ostwaldâ€Ripeningâ€Induced Growth of Parallel Faceâ€Exposed Ag Nanoplates on Microâ€Hemispheres for High SERS Activity. Chemistry - A European Journal, 2013, 19, 9211-9217.	1.7	15
85	Urchin-like Au-nanoparticles@Ag-nanohemisphere arrays as active SERS-substrates for recognition of PCBs. RSC Advances, 2014, 4, 19654-19657.	1.7	15
86	Building desired heterojunctions of semiconductor CdS nanowire and carbon nanotube via AAO template-based approach. Materials Letters, 2009, 63, 2249-2252.	1.3	14
87	Nanocomposite-Decorated Filter Paper as a Twistable and Water-Tolerant Sensor for Selective Detection of 5 ppb–60 v/v% Ammonia. ACS Sensors, 2022, 7, 874-883.	4.0	14
88	SiO2Nanowires Growing on Hexagonally Arranged Circular Patterns Surrounded by TiO2Films. Journal of Physical Chemistry B, 2006, 110, 222-226.	1.2	12
89	Surface-Enhanced Raman Scattering from Au-Nanorod Arrays with Sub-5-nm Gaps Stuck Out of an AAO Template. Journal of Nanoscience and Nanotechnology, 2016, 16, 934-938.	0.9	11
90	Superstructural Raman Nanosensors with Integrated Dual Functions for Ultrasensitive Detection and Tunable Release of Molecules. Chemistry of Materials, 2018, 30, 5256-5263.	3.2	11

#	Article	IF	CITATIONS
91	Ag-coated 3D Cu(OH)2 nanowires on the woven copper mesh as a cost-effective surface-enhanced Raman scattering substrate. Surface and Coatings Technology, 2021, 415, 127132.	2.2	11
92	Efficient electrocatalytic reduction of nitrate to nitrogen gas by a cubic Cu ₂ O film with predominant (111) orientation. Chemical Communications, 2022, 58, 3613-3616.	2.2	11
93	Synthesis and Photoluminescence of Si-Related Nanowires Using Porous Silicon as Si Element Source. Crystal Growth and Design, 2008, 8, 1818-1822.	1.4	10
94	Alumina‧heathed Nanocables with Cores Consisting of Various Structures and Materials. Angewandte Chemie - International Edition, 2011, 50, 2036-2040.	7.2	10
95	A GBI@PPyNWs-based prototype of reusable fluorescence sensor for the detection of Fe3+ in aqueous solution. Analytical Methods, 2012, 4, 2653.	1.3	9
96	R6C/8-AQ co-functionalized Fe3O4@SiO2 nanoparticles for fluorescence detection of trace Hg2+ and Zn2+ in aqueous solution. Science China Materials, 2015, 58, 550-558.	3.5	9
97	Vertically aligned conductive carbon nanotube junctions and arrays for device applications. Applied Physics Letters, 2004, 84, 2889-2891.	1.5	8
98	Synthesis and Thermal Expansion of Copper Nanotubes and Nanowires with Y―and Stepâ€Shaped Topologies. Small, 2010, 6, 381-385.	5.2	8
99	Silver-Nanorod Bundles: A Hierarchically Ordered Array of Silver-Nanorod Bundles for Surface-Enhanced Raman Scattering Detection of Phenolic Pollutants (Adv. Mater. 24/2016). Advanced Materials, 2016, 28, 4870-4870.	11.1	8
100	Na <i>_y</i> WO _{3–<i>x</i>} Nanosheet Array via <i>In Situ</i> Na Intercalation for Surface-Enhanced Raman Scattering Detection of Methylene Blue. ACS Applied Nano Materials, 2022, 5, 7841-7849.	2.4	8
101	Carbon Nanotubes Grafted on Silicon Oxide Nanowires. Journal of Nanoscience and Nanotechnology, 2004, 4, 712-715.	0.9	7
102	Fabrication of hexagonally patterned flower-like silver particle arrays as surface-enhanced Raman scattering substrates. Nanotechnology, 2016, 27, 325303.	1.3	7
103	Fluorescence "turn on―detection of Cr3+ using N-doped-CDs and graphitic nanosheet hybrids. RSC Advances, 2016, 6, 72728-72732.	1.7	7
104	Ordered arrays of Ag nanodendrite clusters as effective surface-enhanced Raman scattering substrates. RSC Advances, 2016, 6, 26490-26494.	1.7	7
105	Surface-enhanced Raman scattering from plasmonic Ag-nanocube@Au-nanospheres core@satellites. Journal of Raman Spectroscopy, 2017, 48, 217-223.	1.2	7
106	Agâ€Nanoparticlesâ€Decorated Geâ€Nanowhisker Grafted on Carbon Fiber Cloth as Flexible and Effective SERS Substrates. ChemistrySelect, 2020, 5, 8338-8343.	0.7	7
107	In-Situ Monitoring the SERS Spectra of para-Aminothiophenol Adsorbed on Plasmon-Tunable Au@Ag Core–Shell Nanostars. Nanomaterials, 2022, 12, 1156.	1.9	7
108	Fluorescent Probes: Well-Defined Nanoclusters as Fluorescent Nanosensors: A Case Study on Au25(SG)18 (Small 13/2012). Small, 2012, 8, 2027-2027.	5.2	6

#	Article	IF	CITATIONS
109	Copper-assisted growth of high-purity carbon nanofiber networks with controllably tunable wettabilities. Journal of Materials Chemistry A, 2021, 9, 22039-22047.	5.2	6
110	Converting Free‣tanding Porous Silicon into Related Porous Membranes. Angewandte Chemie - International Edition, 2008, 47, 365-367.	7.2	4
111	A high performance Li-rich β-Li ₂ IrO ₃ electrode for symmetric lithium ion batteries. Journal of Materials Chemistry A, 2021, 9, 19705-19709.	5.2	4
112	Ultraviolet photoluminescence of porous anodic alumina films. Science Bulletin, 2003, 48, 1090-1092.	1.7	3
113	Synthesis of AuNi/NiO Nanocables by Porous AAO Template Assisted Galvanic Deposition and Subsequent Oxidation. European Journal of Inorganic Chemistry, 2010, 2010, 4309-4313.	1.0	3
114	A facile low-temperature growth of large-scale uniform two-end-open Ge nanotubes with hierarchical branches. Journal of Materials Chemistry C, 2013, 1, 5471.	2.7	1
115	Modulation of optical absorption edge in TiO2/SiO2 mesoporous composites. Science Bulletin, 1998, 43, 2066-2070.	1.7	0
116	Porous Anodic Aluminum Oxide. , 2013, , 859-882.		0
117	Growth kinetics controlled rational synthesis of germanium nanotowers in chemical vapor deposition. Science China Materials, 2015, 58, 877-883.	3.5	0